Science Advances
AAAS

Supplementary Materials for

A zinc-conducting chalcogenide electrolyte

Jian Zhi *et al.*

Corresponding author: Fuqiang Huang, huangfq@mail.sic.ac.cn

Sci. Adv. **9**, eade2217 (2023)
DOI: 10.1126/sciadv.ade2217

This PDF file includes:

Supplementary Discussion 1: Density functional theory (DFT) calculations

Density functional theory (DFT) calculations were conducted employing Vienna Ab-initio Simulation Package (VASP). Perdew-Burke-Ernzerhof (PBE) parameterization of the generalized gradient approximation (GGA) and Ultra-soft (US) pseudopotentials are used for the core-valence electron interaction. The cut-off energy was set as 600 eV. Derived from cubic ZnS, the cell with [1 1 1] as *c*-axis was selected for further optimization with a 6 × 6 × 2 Monkhorst-Pack K-point grid. For F-doped ZnS, a 3 × 3 × 1 supercell was established with a S atom substituted by a F atom and coupled Zn vacancy. A 2 × 2 × 1 K-point grid was used. The Zn-ion probability densities were calculated based on the method of Ceder *et al.* Canonical ensemble was selected with a timestep of 2 fs and 10, 000 steps at 900 K. All the tetrahedral and octahedral sites were filled with Zn atoms in the ZnS and F-doped ZnS model. The probability densities were visualized by python materials genomics (Pymatgen).

DFT was also applied to determine the formation energies of various defects in ZnS. Python Charged Defect Toolkit (PyCDT) package was employed to determine the defect formation energy:

$$E^f[X^q] = E_{tot}[X^q] - E_{tot}[bulk] - \sum_i n_i\mu_i + qE_F + E_{corr} \qquad (1)$$

Here, $E_{tot}[X^q]$and $E_{tot}[bulk]$are the total simulation energy. μ_i and n_i are the chemical potential and number of species I, respectively, and qE_F represents the defect charge multiplied by the Fermi energy at valence band maximum. E_{corr} represents a correction segment corresponding to errors from background charge. All calculations are based on a 3×3×4 supercell of ZnS structure, comprising a total of 278 atoms. The bulk phase was optimised with respect to lattice parameter and atomic positions using an energy cut-off of 600 eV and a 2×2×2 K-point mesh. The lattice geometry was fixed for all additional calculations. Diffusion barriers have been obtained via the climbing image nudged elastic band (NEB) method.

Supplementary Discussion 2: Calculation of transference number

Lithium-ion transference number $t_{Zn^{2+}}$ of Zn-MFZS solid electrolyte was estimated via combination measurements of AC impedance and potentiostatic DC polarization. The DC current as a function of time was measured for Zn/Zn-MFZS/Zn symmetric cells under 10 mV until a steady state was achieved after 1×10^4 s. The cell was also monitored by AC impedance to determine the bulk resistance of Zn-MFZS and Zn-MFZS/Zn interface. The transference number, $t_{Zn^{2+}}$ can thus be obtained by the following equation:

$$t_{Zn^{2+}} = \frac{I(\infty)R_{bulk}(\infty)[\Delta V - I(0)R_{int}(0)]}{I(0)R_{bulk}(0)[\Delta V - I(\infty)R_{int}(\infty)]} \quad (2)$$

where ΔV represents polarization voltage, I represents the current, R_{bulk} and R_{int} are the resistance of the Zn-MFZS and the Zn-MFZS/Zn interface.

Supplementary Discussion 3: Molecular dynamics (MD) simulations

MD simulations were performed in the DL_POLY software. The simulation box contains a ZnS cell replicated 12×12×18 times to obtain a length of 75.24 Å in X–Y plane and 73.65 Å in Z-direction. To simulate pores, ZnS atoms were etched out to obtain a cylinder with a 4 nm (40 Å) in diameter along [010]. The model of porous ZnS contains 2052 atoms, among which there are 1026 Zn atoms and 1026 S atoms. Substitutional fluorine doping was simulated by replacing 57 S atoms with 57 F atoms in this porous ZnS system. Zn^{2+} insertion was realized by loading 10 Zn atoms and 220 OTF^- groups in the cylindrical pore of the system, corresponding to a ZnS/Zn $(OTF)_2$ molar ratio of ≈ 10:1. OTF^- were simulated in the united atom formalism and comprised of one S site connected to three O site and one CF_3 site. 800 dimethylformamide (DMF) molecules

were also added to the simulation system to study the impact of residue DMF in Zn^{2+} conduction. Room temperature (298 K) with a pressure of 1 bar were retained during NPT (constant particle number, pressure and temperature) for 1.0 ns to obtain the density at this stage. Then we removed most DMF molecules to simulate the drying procedure with only 75 DMF molecules left in the system, which is in accordance with the residue DMF concentration as determined from ultrasonic-extraction based GC-MS method. 650 K was employed to accelerate the dynamics. All simulation runs for 6.0 ns were conducted at 650 K under an NVT ensemble employing Nose–Hoover thermostat to investigate the Zn-transport mechanism. Zn^{2+} inserted fluorine doped ZnS system without DMF was also simulated for comparison.

Supplementary Discussion 4: Capacitance calculation

The volumetric energy density (E_{vol}) and power density (P_{vol}) of the device are obtained from the following equations:

$$E_{vol} = \frac{1}{2} \times C_{vol} \times \frac{\Delta V^2}{3600} \quad (3)$$

$$P_{vol} = \frac{E_{vol}}{t} \quad (4)$$

C_{vol} is the volumetric capacitence based the the total volume of solid ZIC, which is calculated from the galvanostatic charge–discharge curves according to the following equation:

$$C_{vol} = \frac{It}{V_T \Delta V} \quad (5)$$

where I is the charging current, t is the discharge time, V_T is the total volume of the solid ZIC device (0.6 cm^3, including 0.28 cm^3 NDFLC@Zn-MFZS, 0.29 cm^3 Zn-MFZS and 0.028 cm^3 Zn foil), and ΔV is the voltage drop opon discharging.

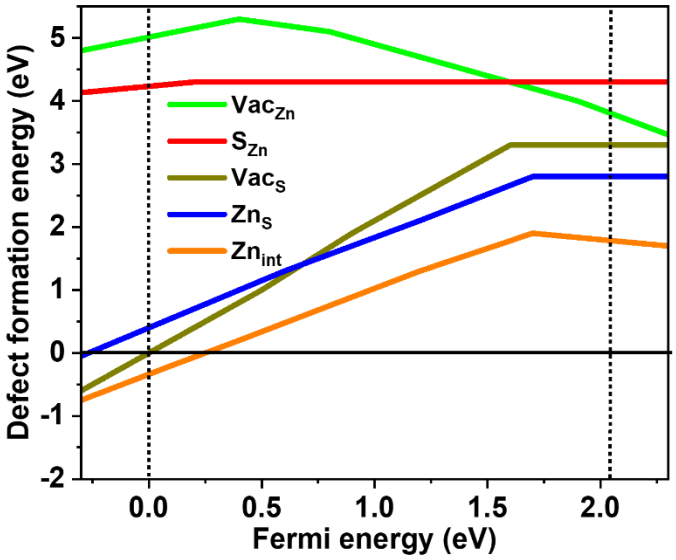

Figure S1. Formation energies of various defects in a 3×3×4 ZnS supercell. Vac_{Zn} and Vac_S are Zn and a S vacancy, respectively; Zn_{inter} is an interstitial Zn atom, S_{Zn} and Zn_S are antisite defects with a S atom on a Zn and vice versa, respectively.

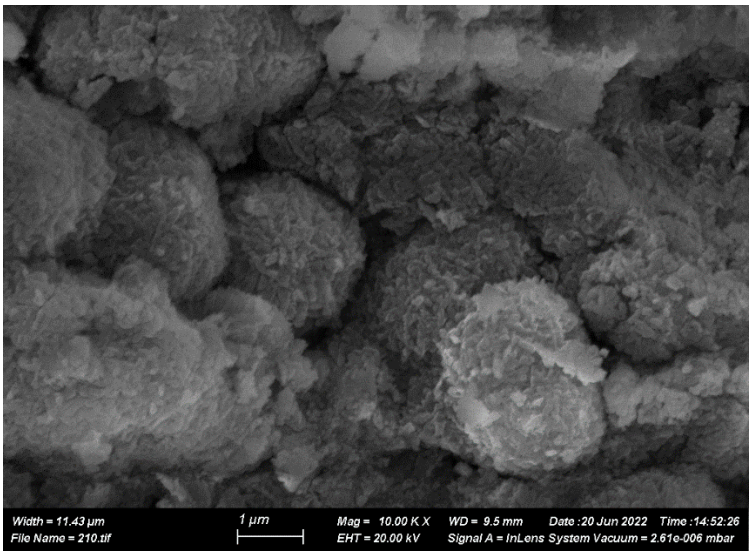

Figure S2. SEM image of MFZS sample.

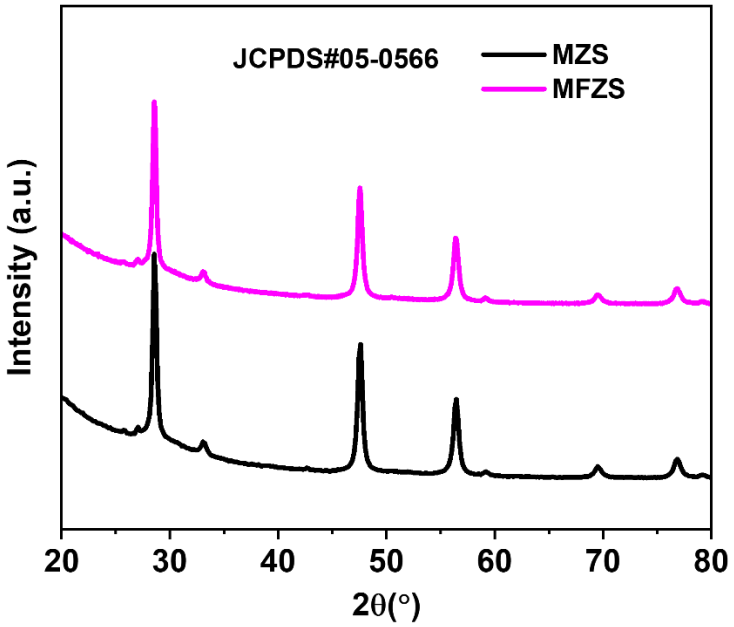

Figure S3. XRD patterns of MZS and MFZS samples

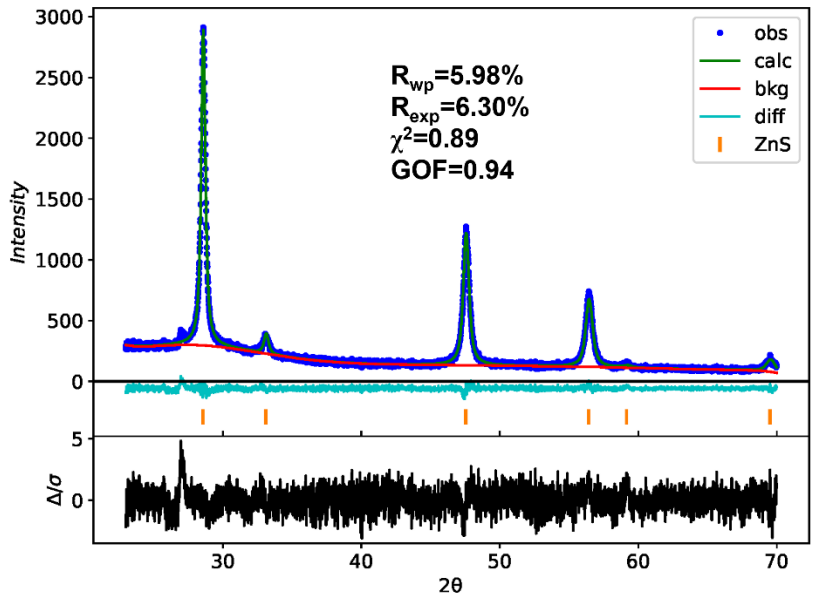

Figure S4. Rietveld refinement XRD spectra for MFZS (5.6 at% fluorine). The experimental XRD data (obs) are fitted with theoretical data (calc). The difference between the experimental and calculated intensities (diff) is plotted below the simulated pattern. "bkg" is the background model used for the Rietveld refinements. Black curves in the bottom represent the magnified difference ("diff" curves, light blue) between the measured and the calculated intensities.

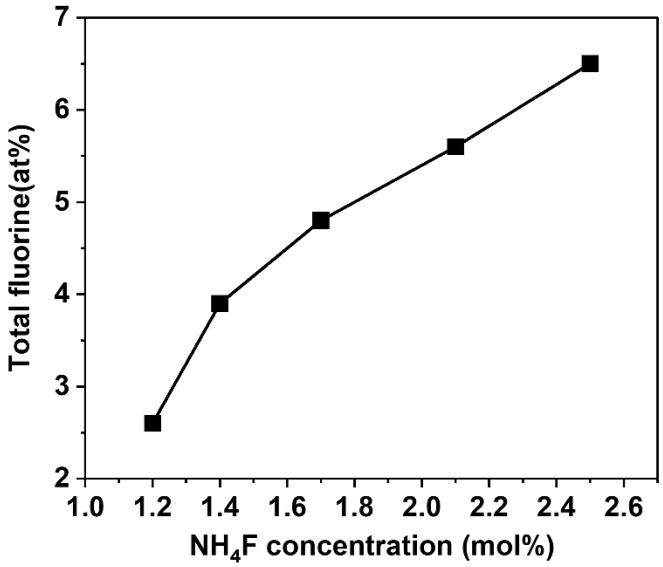

Figure S5. Correlation between NH_4F concentration in the initial EISA sol and total fluorine in MFZS samples

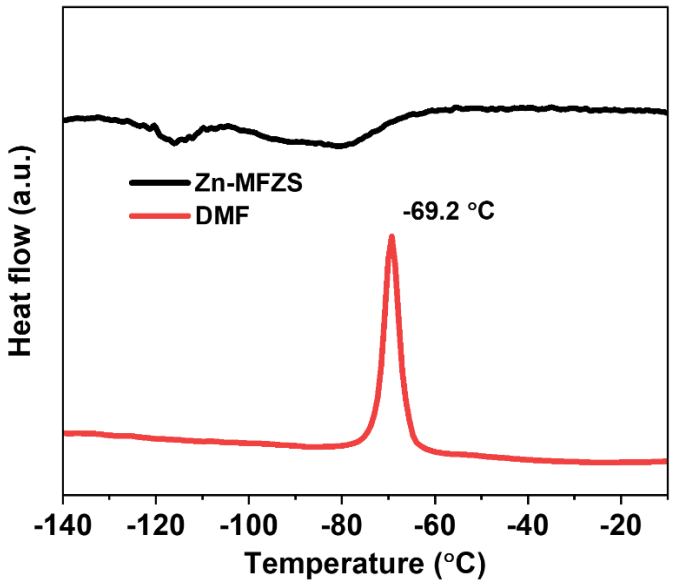

Figure S6. DSC for Zn-MFZS and pure DMF down to -140 °C (Hold for 10 minutes) at a rate of 5 °C min^{-1} with simultaneous liquid nitrogen cooling and scanned from -140 °C to -10 °C at a rate of 5 °C min^{-1}

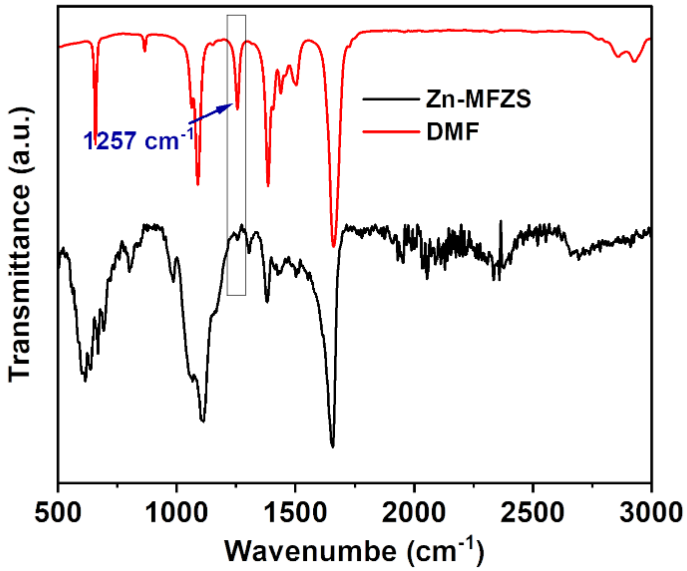

Figure S7. FTIR spectrum of Zn-MFZS and DMF

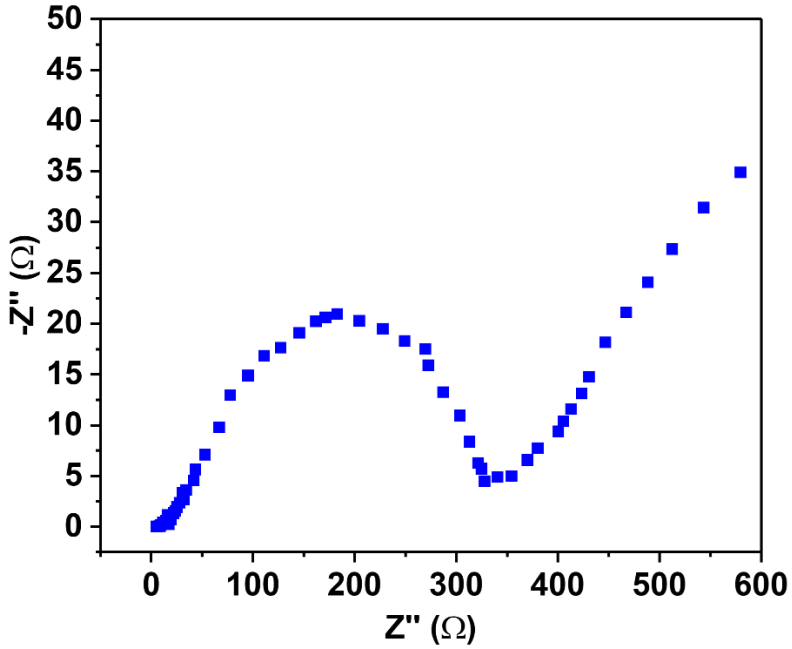

Figure S8. Nyquist of Zn-MFZS at 25 °C

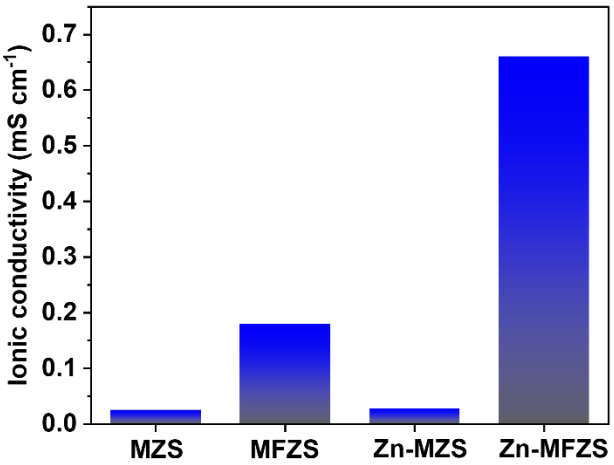

Figure S9. Ionic conductivity of MZS, MFZS, Zn-MZS and Zn-MFZS.

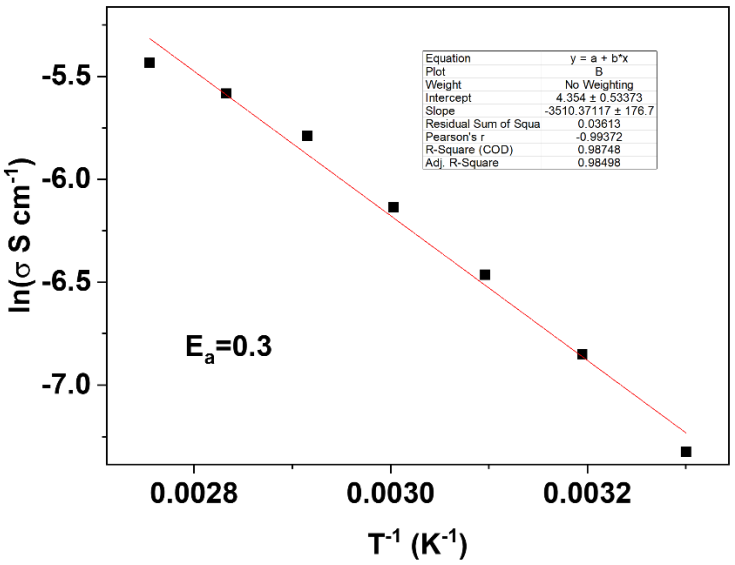

Figure S10. Details for the calculation of active energy for Zn-MFZS.

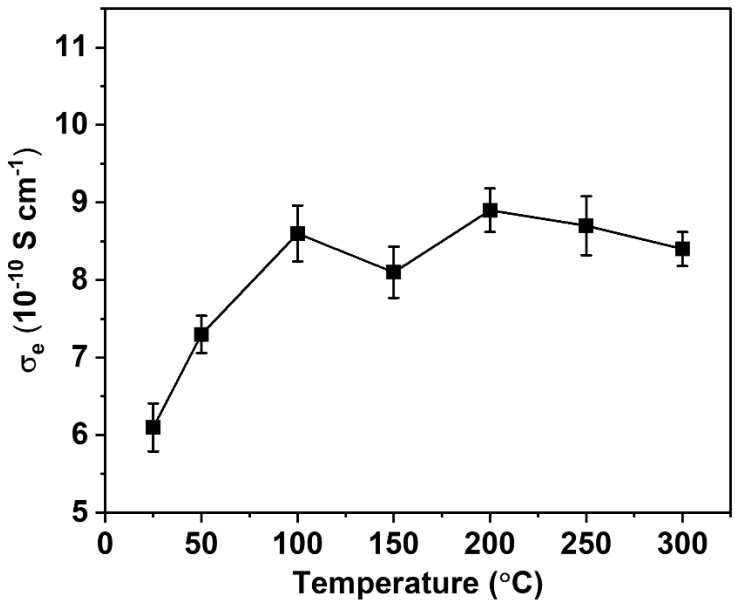

Figure S11. Electronic conductivity Zn-MFZS at 25-300 °C.

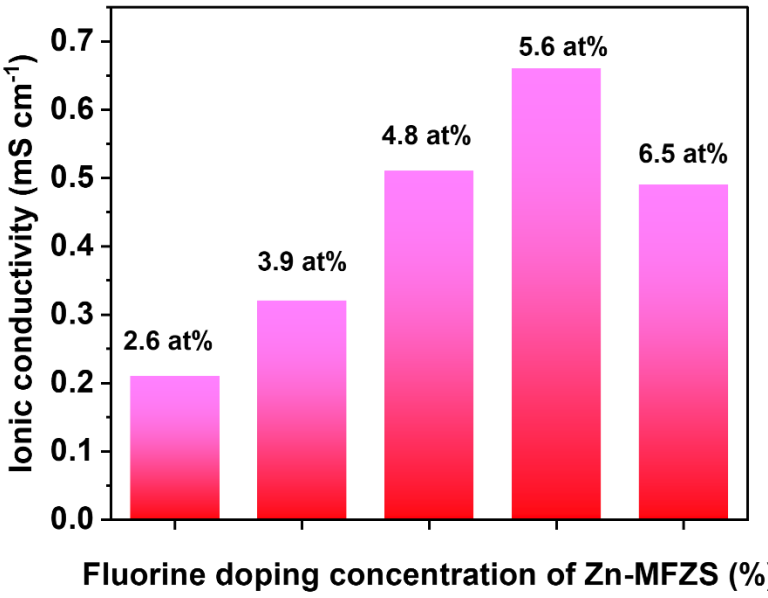

Figure S12. Ionic conductivity of Zn-MFZS with different fluorine doping concentrations.

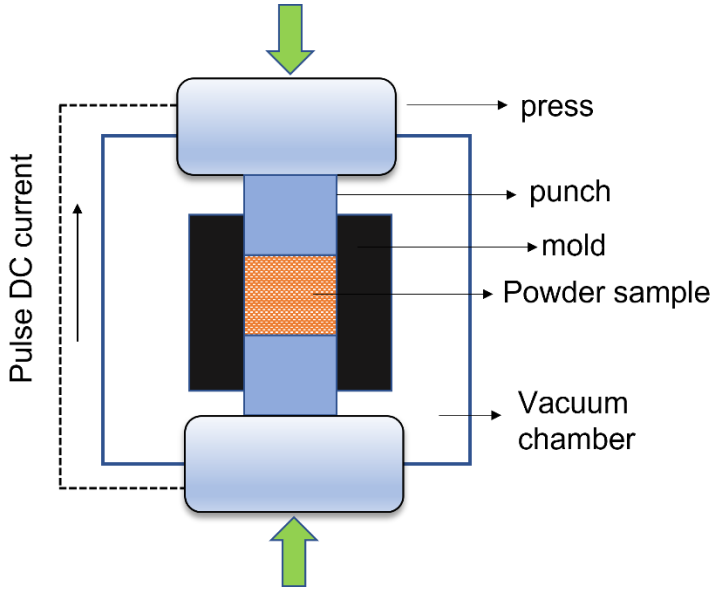

Figure S13. Components of SPS apparatus.

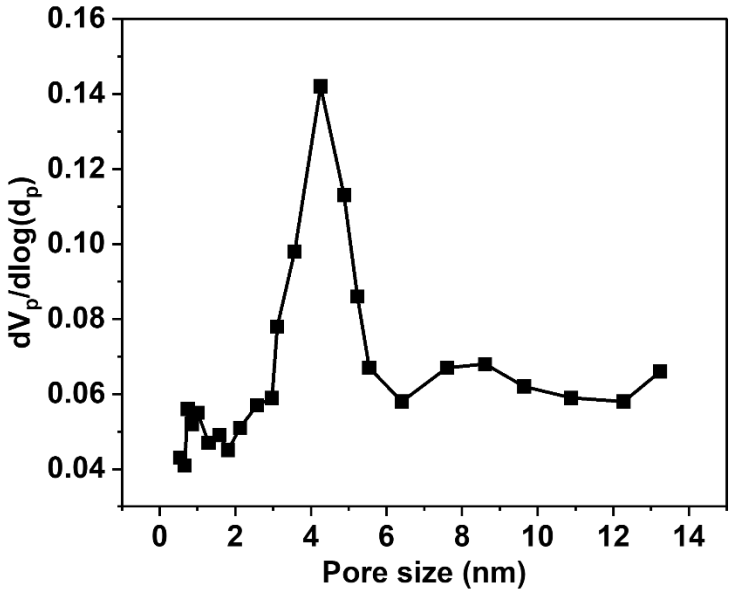

Figure S14. Pore size distribution of Zn-MFZS^{SPS}.

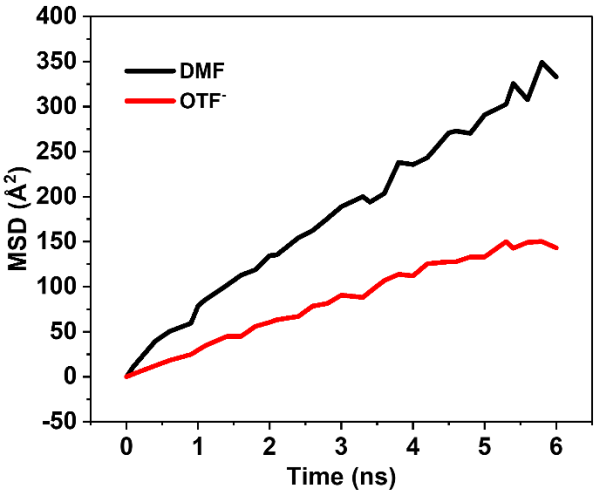

Figure S15. MSD of DMF and OTF^- in fluorine doped ZnS systems with 110 OTF^- ions + 75 DMF molecules.

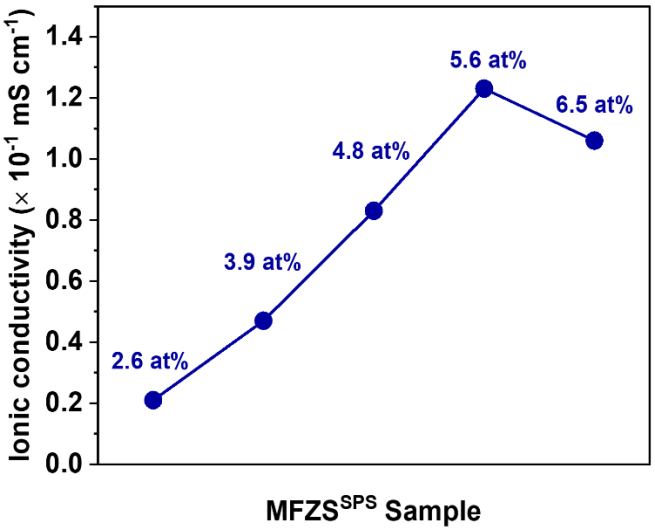

Figure S16. Ionic conductivity of $MFZS^{SPS}$ with different fluorine doping concentrations.

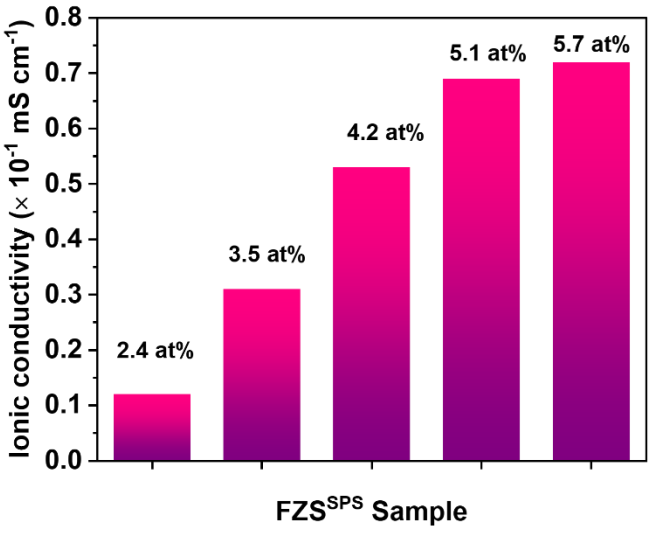

Figure S17. Ionic conductivity of FZS^{SPS} with different fluorine doping concentrations.

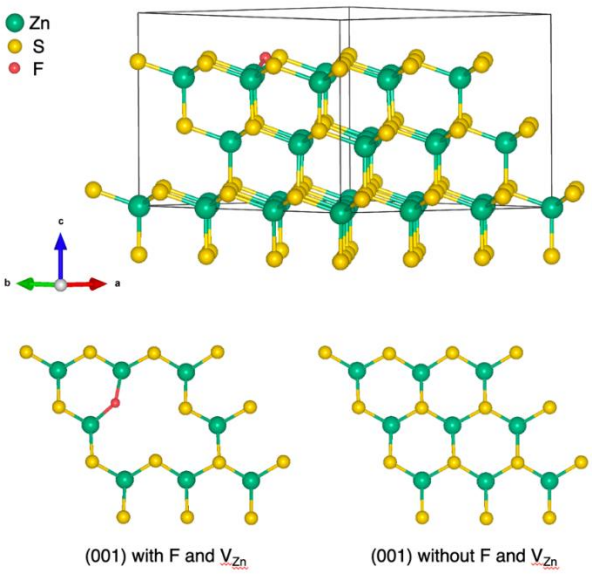

Figure S18. The cell model of F-doped ZnS with Zn vacancy (V_{Zn}). The (001) planes with and without F and V_{Zn} are shown in the lower part.

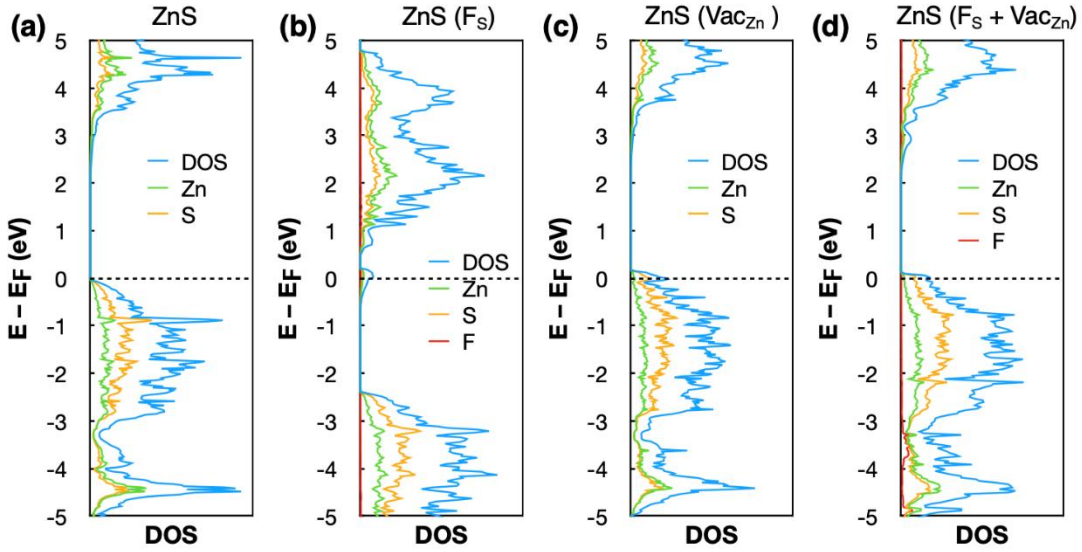

Figure S19. The density of states (DOS) for ZnS. (a), ZnS with F_S (b), or ZnS with Vac_{Zn} is (c) and ZnS:F (d).

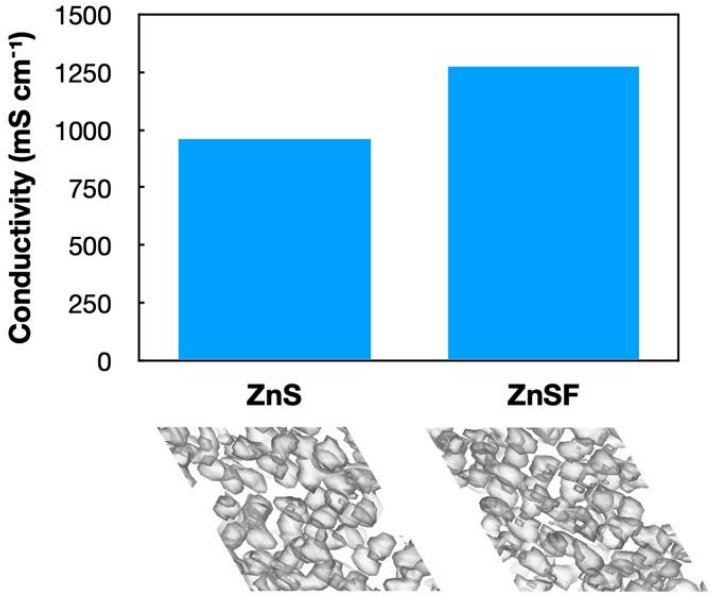

Figure S20. The conductivity of ZnS and F-doped ZnS based on AIMD at 900 K. The inset below is the probability density of correlated cell.

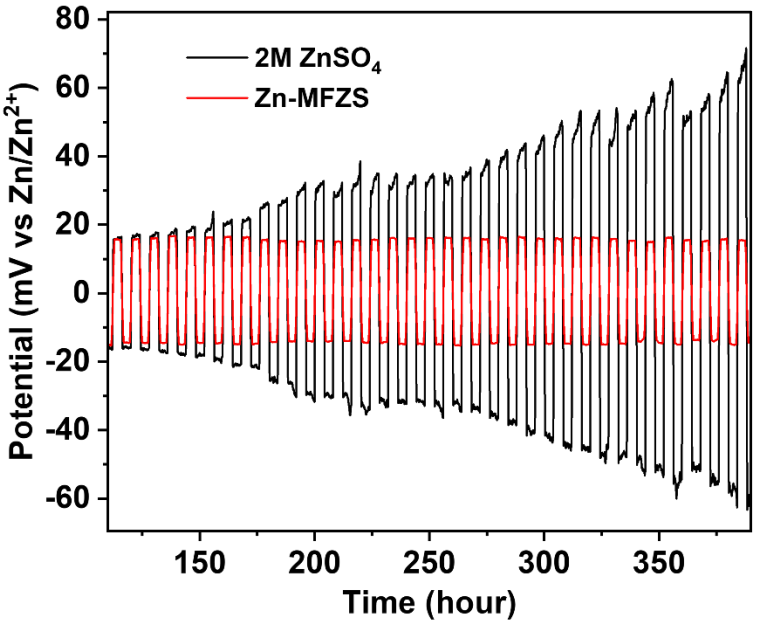

Figure S21. Enlarged details of Figure 3a (from 110 to 390 hours).

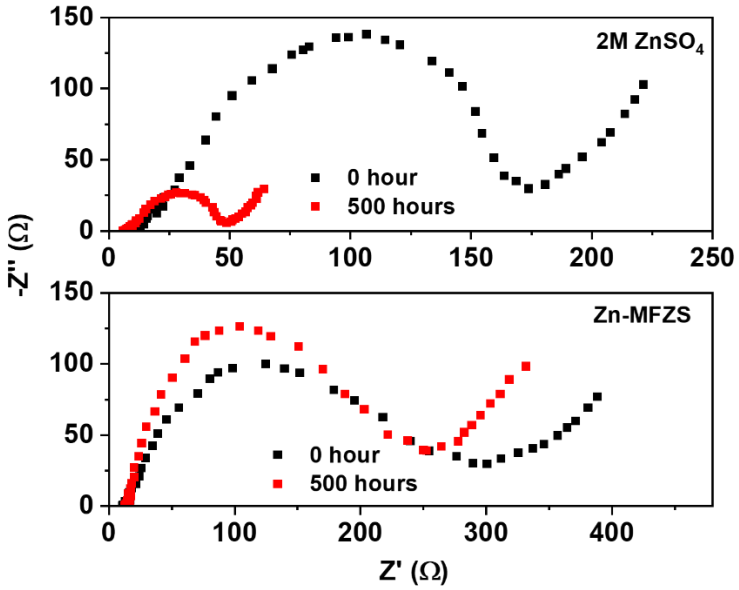

Figure S22. Nyquist plots of Zn/Zn symmetric cells with aqueous electrolyte (2M $ZnSO_4$) and solid electrolyte (Zn-MFZS) before and after 500 hours cycling.

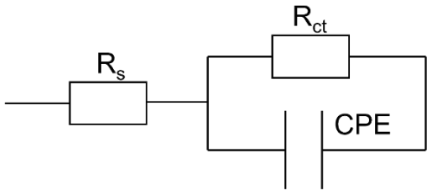

Figure S23. Equivalent circuit for the Nyquist plot fitting of symmetrical cells.

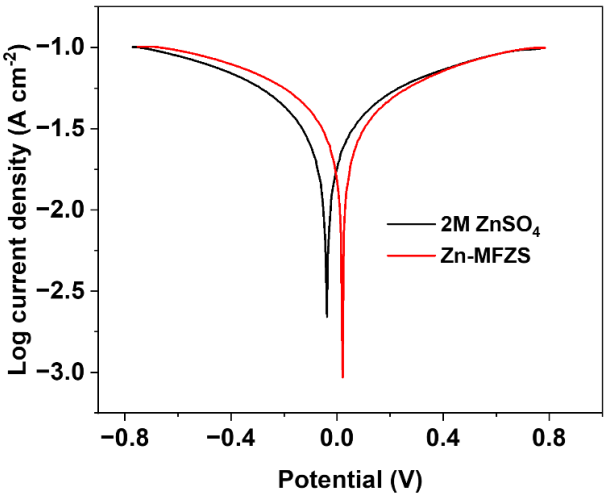

Figure S24. Linear polarization curves of Zn/Zn symmetrical cells with aqueous and Zn-MFZS electrolyte.

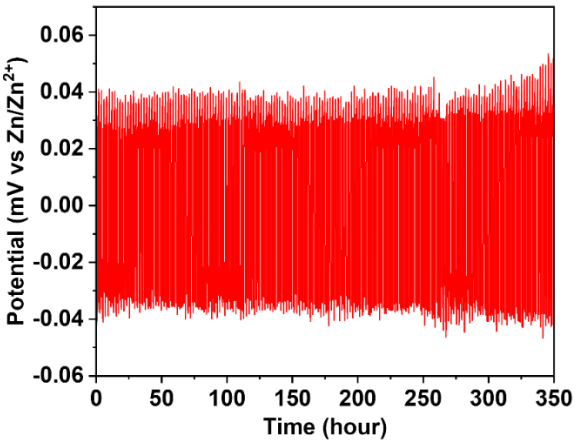

Figure S25. Zn plating/stripping performance of Zn/Zn symmetric cell with Zn-MFZS under 10 mA cm^{-2} with a 10 mAh cm^{-2} per-cycle areal capacity.

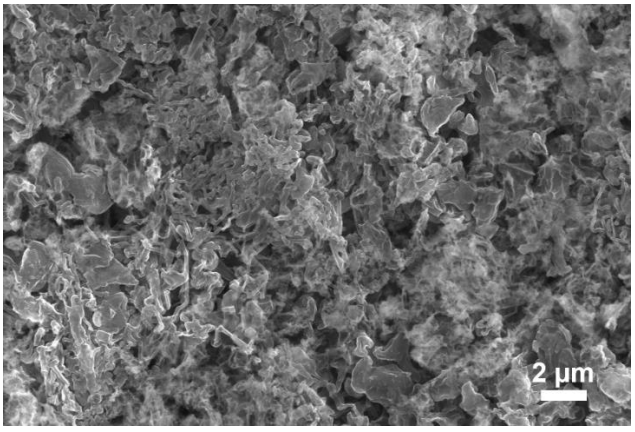

Figure S26. SEM images of Zn anode in symmetric cell with Zn-MFZS electrolyte after long-term cycling for 350 hours at 10 mA cm^{-2}.

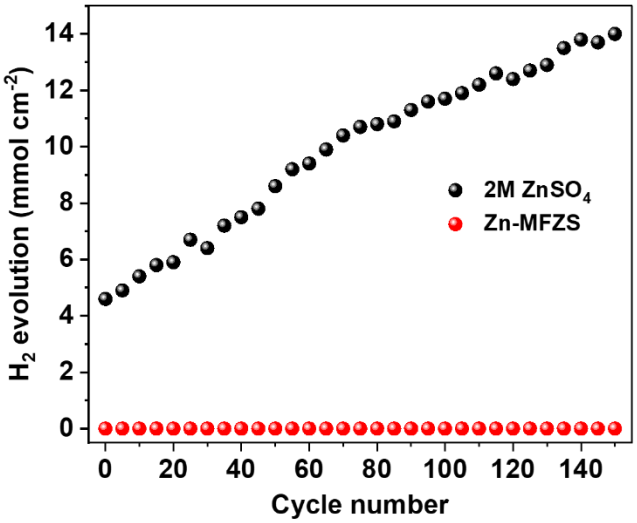

Figure S27. Hydrogen production of Zn/Zn symmetric cell with aqueous electrolyte (2M $ZnSO_4$) and solid electrolyte (Zn-MFZS) during Zn plating/stripping process at current density of 0.2 mA cm^{-2}.

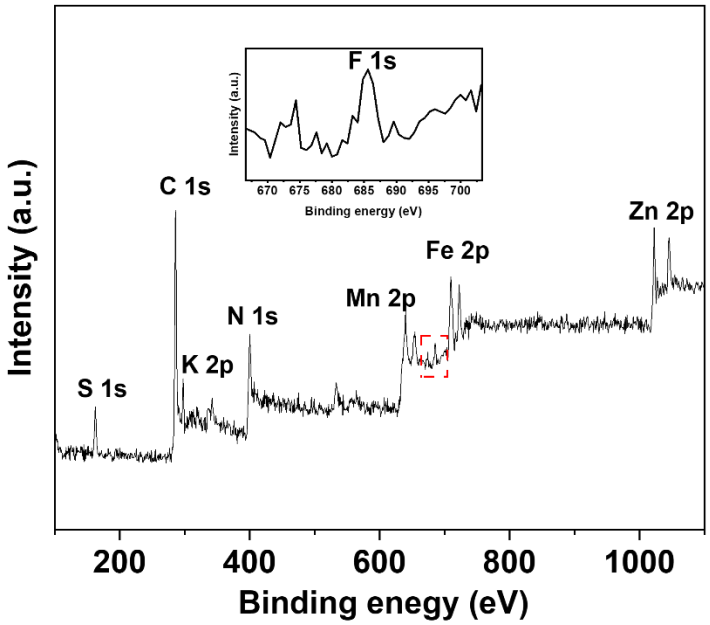

Figure S28. XPS survey spectrum of MnHCF grown on MFZS matrix.

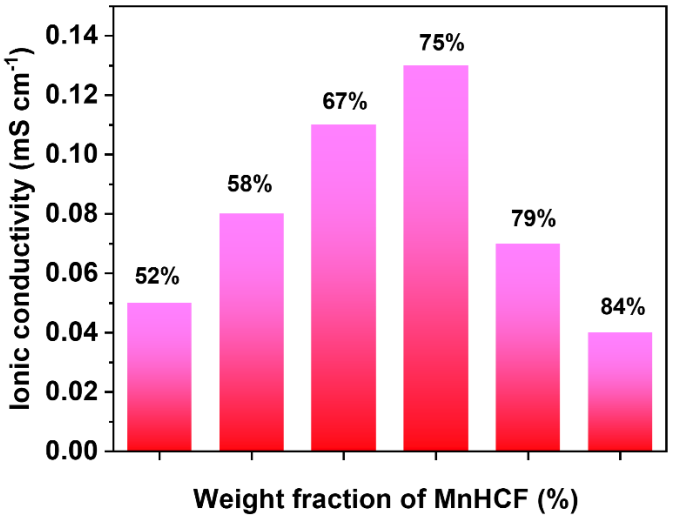

Figure S29. The ionic conductivity of MnHCF@Zn-MFZS integrated cathodes with different weight fraction of MnHCF.

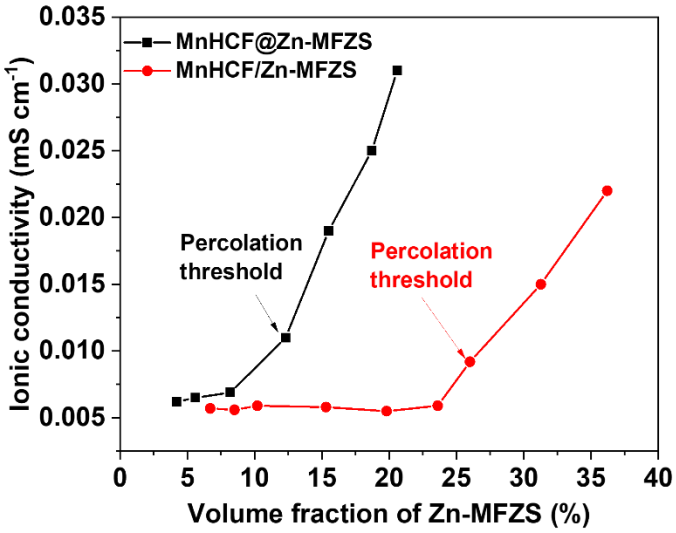

Figure S30. Ionic conductivity of MnHCF@Zn-MFZS and MnHCF/Zn-MFZS cathodes made with different amounts of Zn-MFZS to achieve ionic percolation.

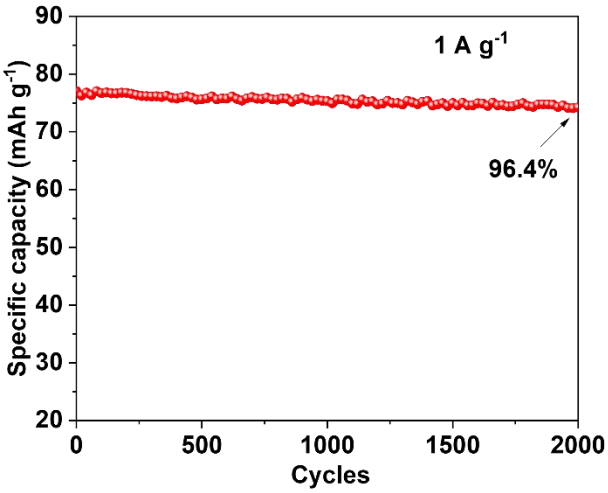

Figure S31. Cycling performance of solid ZIB with Zn-MFZS electrolyte at 1 A g^{-1}.

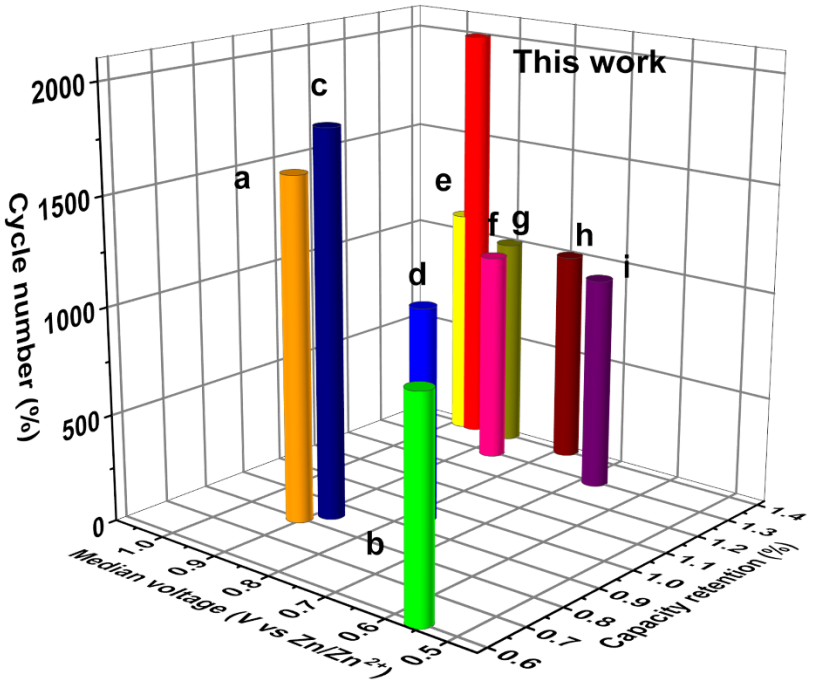

Figure S32. Contrast of cycling stability between solid ZIB with Zn-MFZS electrolyte and state-of-the-art optimized aqueous Zn-ion batteries under the same rate (1 A g^{-1}): a(Ref.34), b(Ref.39), c(Ref.40), d(Ref.37), e(Ref.35), f(Ref.36), g(Ref.41), h(Ref.33), i(Ref.38).

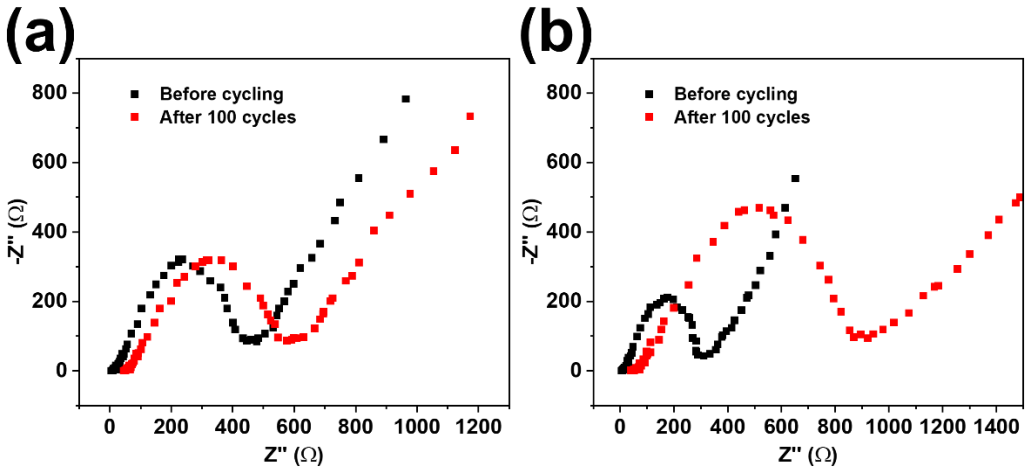

Figure S33. **Galvanostatic electrochemical impedance spectroscopies in full cells.** (a,b) Nyquist plot of full cells with aqueous (a) and Zn-MFZS (b) electrolyte before and after cycling.

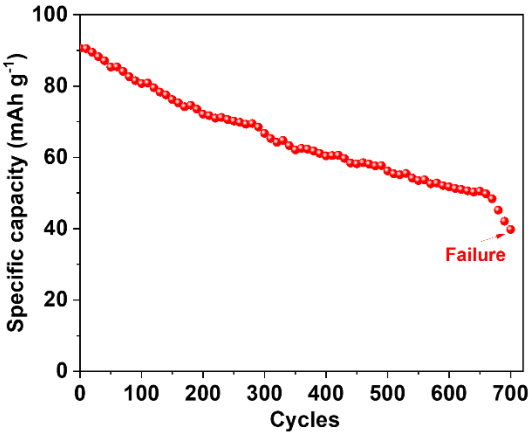

Figure S34. Cycling performance of quasi-solid ZIB employing non-mesoporous fluorine doped ZnS as electrolyte (Zn-FZS) and MnHCF@Zn-FZS as cathode, with a DMF concentration over 40 mol% in Zn-FZS.

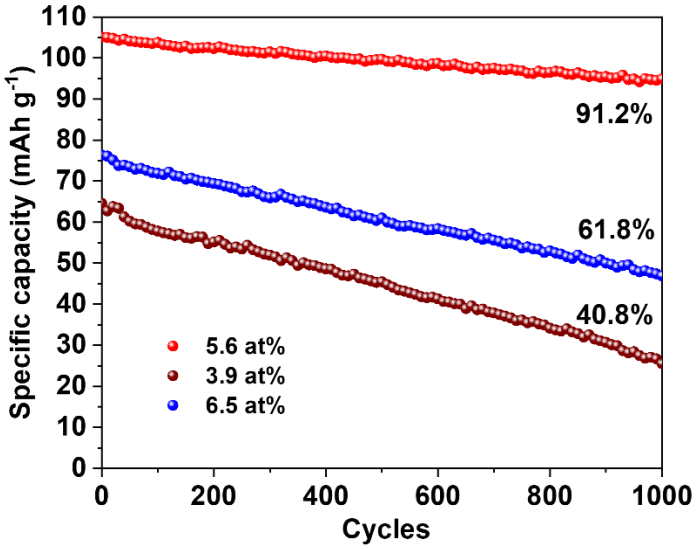

Figure S35. Cycling performance of Zn-MFZS based solid ZIB with various fluorine doping concentrations at 1C.

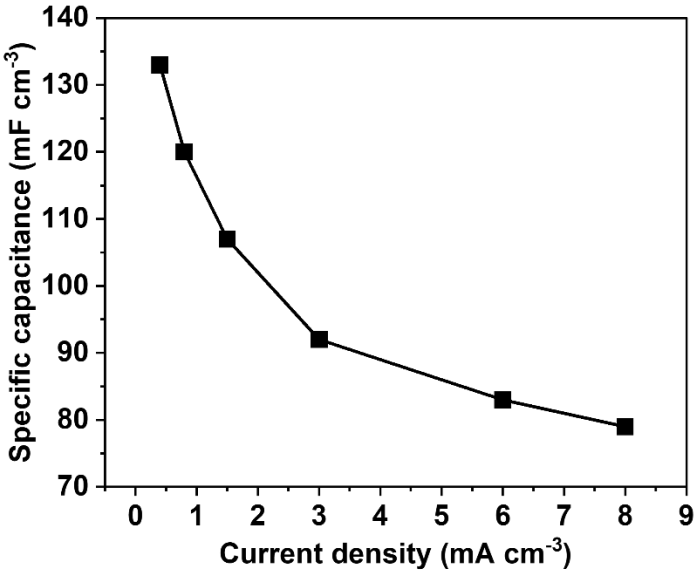

Figure S36. Specific capacitance of assembled solid ZIC (NDFLC@Zn-MFZS as positive electrode, Zn-MFZS as solid electrolyte and Zn foil as negative electrode) under different current densities.

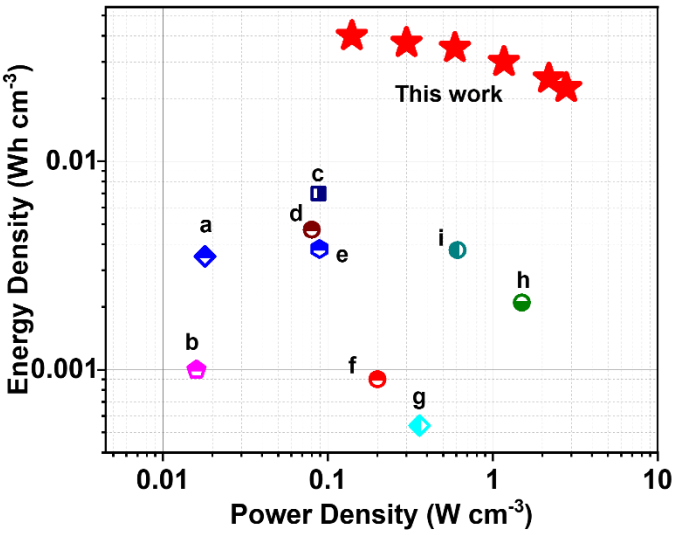

Figure S37. Ragone plot of solid ZIC in this work in comparison with some recent reported ZICs: a(Ref.48), b(Ref.49), c(Ref.50), d(Ref.51), e(Ref.52), f(Ref.53), g(Ref.54), h(Ref.55), i(Ref.56).

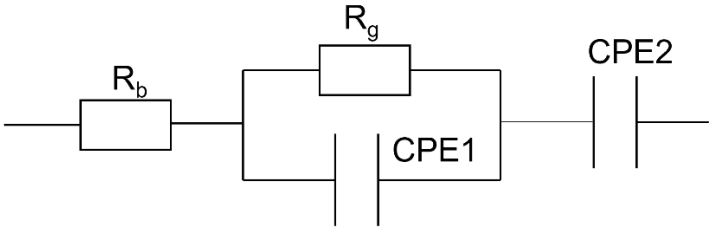

Figure S38. Equivalent circuit for the Nyquist plot fitting of Zn-MFZS, Zn-MFZSe and Zn-MFZTe electrolyte. R_b and R_g represents the bulk impedance and crystalline grain impedance, respectively.

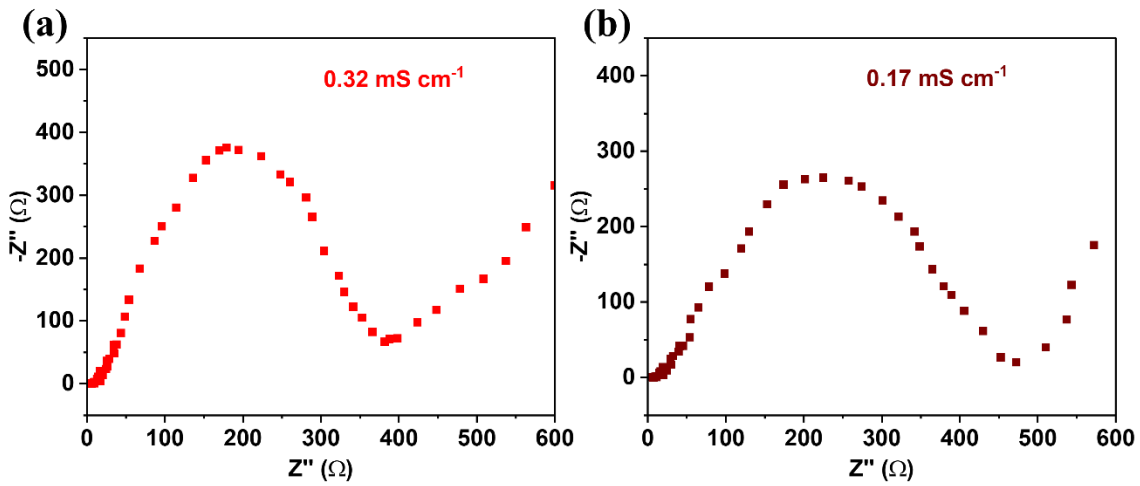

Figure S39. **Galvanostatic electrochemical impedance spectroscopies of Zn-MFZSe and Zn-MFZTe electrolyte.** (a,b) Nyquist plot of Zn-MFZSe (a) and Zn-MFZTe (b) at 25°C.

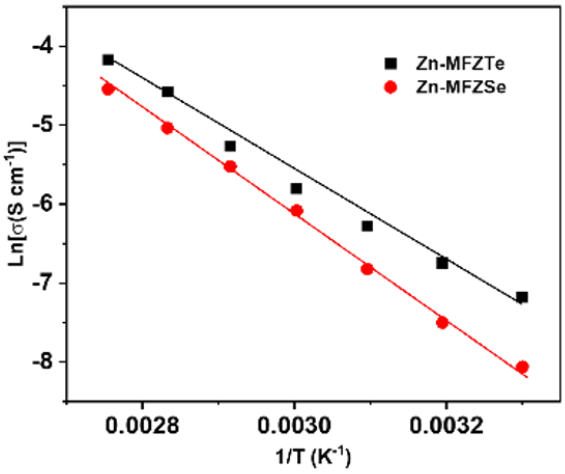

Figure S40. Temperature-dependent conductivity of Zn-MFZSe and Zn-MFZTe with linear fitting according to the Arrhenius equation.

Table S1 Refined structural parameters for MFZS from X-ray diffraction data

Atom	Wyckoff position	x	y	z	Occupies
Zn	4a	0	0	0	0.868
S	4d	0.25	0.25	0.75	0.913
F	4d	0.25	0.25	0.75	0.015

Table S2. Lattice parameters and crystallite size of MFZS samples with different fluorine doping concentration.

Fluorine (at%)[a]	Lattice parameters				Crystallite size (nm)
	a(Å)	b(Å)	c(Å)	V(Å)^3	
0	5.3702	5.3702	5.3702	154.87	207
2.6	5.3621	5.3621	5.3621	154.17	205
3.9	5.3545	5.3545	5.3545	153.52	196
4.8	5.3436	5.3436	5.3436	152.58	194
5.6	5.3361	5.3361	5.3361	151.94	193
6.5	5.3308	5.3308	5.3308	151.49	190

[a] Obtained from XPS analysis

Table S3. Fluorine distribution and porosity various MFZS samples

Fluorine (at.%)[a]	%F_{sur}	%F_{sub}	S_{BET} (m^2 g^{-1})[b]	Pore size (nm)[b]
2.6	0.1	2.5	242	4.42
3.9	0.3	3.6	224	4.51
4.8	0.4	4.4	263	4.33
5.6	0.6	5.0	257	4.58
6.5	1.6	4.9	219	4.24

[a] Obtained from XPS analysis
[b] Obtained from nitrogen sorption isotherm

Table S4. Diffusion coefficients ($\times 10^{-7}$ cm^2 s^{-1}) of Zn^{2+}, OTF^- and DMF in different fluorine doped ZnS systems

Systems	Zn^{2+}	OTF^-	DMF
0 OTF^-+0 DMF	0.12	N/A	N/A
110 OTF^-+0 DMF	0.47	0.51	N/A
110 OTF^-+75DMF	1.10	1.22	9.25

[a] The diffusion coefficient D is calculated by D=MSD/6t, where the MSD values are taken from MSD plots of various systems (e.g. Figure S11), and t is the simulation time.

Table S5. Comparison between calculated F-doped ZnS and 3 × 3 × 1 ZnS supercell parameters.

Parameters	F-doped ZnS	ZnS
a (Å)	11.55601	11.56177
b (Å)	11.55601	11.56177
c (Å)	9.37543	9.44014
α (°)	89.7008	90.0000
β (°)	90.2992	90.0000
γ (°)	120.5371	120.0000

Table S6. Fitting result for the Nyquist plot of aqueous and Zn-MFZS based Zn/Zn symmetric cells before and after cycling (Figure SX)

Sample	R_s (Ω)	R_{ct} (Ω)	CPE
Aqueous Zn/Zn symmetric cell	12.67	154.36	37.21
Aqueous Zn/Zn symmetric cell (500 hours cycling)	7.34	47.28	33.65
Zn-MFZS based Zn/Zn symmetric cell	14.51	247.18	29.72
Zn-MFZS based Zn/Zn symmetric cell (500 hours cycling)	13.65	226.54	26.39

Table S7. Gas flow conditions and corresponding material properties of various NDFLC@Zn-MFZS samples

Sample	Flow concentration (sccm)				Material Properties			
	Ar	CH_4	H_2	NH_4	Carbon content (wt%)[a]	N content (at%)[b]	Ionic conductivity (mS cm^{-1})	Electrical conductivity (mS cm^{-1})
S1	300	10	20	20	12.7	3.6	0.026	0.0217
S2	300	10	20	40	14.3	5.2	0.049	0.0531
S3	300	10	20	60	16.8	7.4	0.088	0.0772
S4	300	10	20	80	15.4	8.7	0.132	0.0919
S5	300	10	20	100	17.5	9.2	0.161	0.1038
S6	300	20	20	100	26.3	8.8	0.154	0.1054
S7	300	40	20	100	38.2	7.5	0.086	0.2178
S8	300	60	20	100	47.8	6.4	0.052	0.3802
S9	300	80	20	100	56.5	5.1	0.043	0.3391
S10	300	100	20	100	71.7	3.9	0.028	0.3062

[a] Determined from TGA
[b] Based on XPS analysis

Table S8. Fitting result for the Nyquist plot of Zn-MFZS, Zn-MFZSe and Zn-MFZTe electrolyte (Figure S8 and S38).

Sample	R_b (Ω)	R_g (Ω)	CPE1	CPE2
Zn-MFZS	5.36	342.34	0.387	11.36
Zn-MFZSe	4.29	382.71	0.672	19.72
Zn-MFZTe	7.92	451.27	0.327	27.42